Theoretical prediction and direct observation of the hot molecules of pyrazolotriazole azomethine dyes by steady state fluorescence

Denis Kondakov *

Imaging Materials & Media, R&D, Eastman Kodak Company, Rochester, NY 14650-02103, USA

Received (in Cambridge, UK) 14th December 2000, Accepted 4th April 2001
First published as an Advance Article on the web 9th May 2001

Pyrazolotriazole (PT) azomethine dyes in the S_1 electronic state were studied by emission spectroscopy and *ab initio* CI-singles and MCSCF methods. Electronically excited molecules are predicted to follow a barrierless relaxation trajectory involving a twisting of the arylamino fragment. Conformational searching yielded the only minimum on the CI-singles S_1 potential energy surface (PES), with characteristic features being a twisted geometry and small S_1–S_0 gap (<0.3 eV). These features preclude its assignment to an experimentally observed fluorescent state (FS) characterized by the emission maximum at 550–600 nm. It is suggested that the FS is a non-Boltzmann population of vibrationally hot molecules with near-planar geometry in a relatively flat region of the S_1 PES. The predicted nonclassical nature of the FS coincides with a remarkable observation of the unprecedented dependence of the fluorescence spectra on the excitation wavelength. In excellent agreement with computational models, a shift of the excitation towards longer wavelengths results in an emission band shift of comparable magnitude along with a significant decrease in a relative fluorescence quantum yield.

Introduction

Characterization of the excited singlet states of pyrazolotriazole (PT) azomethine dyes is of considerable importance in view of their extensive use as photographic image-forming magenta dyes. The 7*H*-pyrazolo[5,1-*c*][1,2,4]triazole skeleton, **1** (Fig. 1), was first introduced by Bailey to take advantage of the

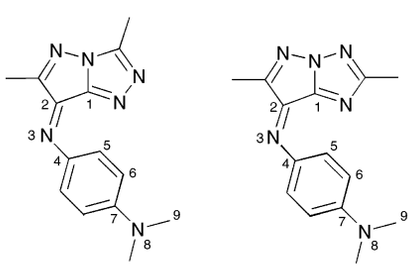

1 **2**

Fig. 1 Molecular structures and atom numbering of the PT dyes.

excellent color reproduction properties of the respective dyes in a subtractive color system.[1] Their particularly noteworthy feature is a negligible unwanted secondary absorption in the blue region. The isomeric skeleton, 7*H*-pyrazolo[1,5-*b*][1,2,4]-triazole, **2**, was also reported to bring forth comparable magenta dyes.[2] Both dye types typically exhibit a high absorption coefficient and an oscillator strength approaching unity. Such absorption spectrum features are likely to result from the planar structure assumed by the PT dyes in the ground state as demonstrated by X-ray crystallography[3] and *ab initio* quantum chemical calculations.[4]

Whereas the structure and properties of the ground state of PT dyes appear to be relatively well understood, very little conclusive evidence for the excited singlet state structures is available. In terms of their photochemical behavior, PT dyes have proved to be puzzling molecules. Only a few studies dealing with excited singlet state properties of PT dyes have been published. Steady state fluorescence measurements reported by Douglas reveal structureless emission with a quantum yield of *ca.* 10^{-4} at room temperature in low viscosity solvents.[5] Low temperature and high viscosity conditions were reported to lead to a considerable increase in the fluorescence quantum yield.[6] A relatively small Stokes shift of the fluorescence observed for both classes of PT dyes can be taken as an indication of the similarity between the ground and excited state geometries. Accordingly, similar oscillator strengths may be expected for the emission and absorption. Based on these assumptions, a lifetime of *ca.* 10 ps for the fluorescent state can be estimated from the fluorescence quantum yield at a room temperature in glycerol–ethanol (96 : 4), which is in good order-of-magnitude agreement with the results of the direct lifetime measurements using the photon-counting method.[6] However, the lifetime measurements were reported to yield nonmonoexponential fluorescence decays, which required two or three exponentials to attain a satisfactory fit. It should be noted that, although this seemingly implies the involvement of two or three separate fluorescent transients, other interpretations might be equally plausible. Furthermore, it is known that the lifetimes obtained from nonmonoexponential decays may not even have any physical significance.[7] Even more puzzling is the pronounced mismatch between changes in fluorescence quantum yields and changes in fluorescent lifetimes, which may imply partitioning between several short-lived transients.[6]

Several groups have applied picosecond absorption recovery techniques to study excited singlet states of PT dyes.[6,8] Unlike the fluorescence lifetime measurements, the absorption recovery techniques permit the detection and lifetime measurement of nonfluorescent transients. Although, in principle, both fluorescent and nonfluorescent transients can be detected, their assignment has proven to be ambiguous for the PT dyes. Interestingly, multiexponential kinetics of the absorption recovery sensitive to the probe wavelength were generally observed, which had been interpreted in terms of several transients of obscure nature formed either sequentially or in parallel.

To sum up, despite the considerable experimental efforts by means of a variety of absorption and emission spectroscopic techniques, conclusive evidence for the excited singlet state structures of PT dyes is still lacking. On the other hand, substantial progress in the development of the theoretical methods

DOI: 10.1039/b010165f

applicable to excited state calculations, particularly *ab initio* methods such as CI-singles, multiconfigurational self-consistent field (MCSCF), and coupled-cluster has been achieved in the past decade.[9] These methods have proved to be quite useful in elucidating photochemical reactions.[10] For the PT dyes, the lowest singlet excited state has been briefly examined using semiempirical PM3-CI[11] and *ab initio* CI-singles[12] methods. However, such calculations frequently yield several different models describing a given photochemical reaction. Thus, the assignment of the excited state structures and information about photochemical reaction mechanisms can only be successfully obtained by experimental and theoretical efforts in conjunction. In the present study we have used steady state fluorescence in conjunction with CI-singles and MCSCF computational methods to study the nature and behavior of the excited singlet state of PT dyes.

Experimental

Materials

Dye **1** was prepared by an oxidative coupling reaction of dimethylaminoanilinium developer and the corresponding pyrazolotriazole coupler, which was provided by R. Jain. Purification by column chromatography and subsequent recrystallization from ethyl acetate–methylene chloride yielded a sample of the dye with at least 99.95% purity by HPLC/UV–Vis. Sucrose octaacetate, obtained from Aldrich, was recrystallized twice from ethanol before use. Ethyl acetate of spectrophotometric grade was obtained from EM Science and used without further purification.

Spectroscopic techniques

Absorption spectra were measured with a Hewlett Packard 8452A UV–Vis spectrophotometer. Fluorescence spectra were measured with a Spex Fluorolog-3 spectrofluorimeter. In all experiments, the fluorescence was collected from the sample at a right angle with respect to the excitation light, and the appropriate corrections for the instrument response were made. Fourier smoothing was performed during the processing of spectra. Samples with absorption lower than 0.15 were used for the fluorescence measurements.

Computational details

Gamess[13] and PC Gamess[13,14] programs were used for the ground state calculations at the HF/6-31G*, HF/6-31+G*, HF/6-31++G**, and MP2/6-31G* levels and for the singlet excited state calculations at the MCSCF and MCQDPT levels with various active spaces. Tight convergence criteria (0.00001) were used in geometry optimizations that were followed by vibrational analysis. MCSCF vibrational frequencies were calculated numerically, using the 4×10^{-7} convergence criterion for maximum asymmetry in the Lagrangian matrix. Excitation energies were obtained as energy differences between the S_0 and S_1 states that had undergone separate orbital optimizations. Oscillator strengths were calculated using orbitals obtained in state-averaged calculations. CIS/6-31G* excited state calculations were performed with the Gaussian 98 program.[15] Loose convergence criteria were used in constrained geometry optimizations. Tight convergence criteria were used in geometry optimizations that were followed by vibrational analysis. CI-singles vibrational frequencies were calculated analytically. Single point CIS/6-31+G* and CIS/6-31++G** calculations were performed with PC Gamess using a (51,120) orbital window.

Results and discussion

In order to elucidate structures of the possible excited singlet state transients, Monte-Carlo conformational searching was performed. Full optimizations of **1** and **2** using the RHF/6-31G* method yielded starting geometries **1a** and **2a** (Table 1). For both structures, CI-singles calculations predicted that the lowest transition has a π–π^* nature and is dominated by HOMO $\longrightarrow$ LUMO single excitation. Despite the localization of HOMO and LUMO orbitals mostly on different rings, this electronic transition has a high oscillator strength ($f > 1$) and might be therefore assigned to the dominant absorption band in the experimental ultraviolet and visible spectrum. Thus, in the subsequent calculations, S_1 was chosen as the state of interest. At each step of the conformational searching the torsions C1–C2–N3–C4, C2–N3–C4–C5 and C6–C7–N8–C9 were varied randomly, followed by a complete geometry optimization using the CI-singles method. The identified S_1 state minima were used as starting points for the subsequent steps of the conformational searching. As was expected by analogy with simple molecules such as formaldimine, the global minima were found to correspond to the twisted geometries given in Table 1 as **1b** and **2b**. Interestingly, no additional minima on the S_1 potential energy surface were located. Vibrational analysis of **1b** confirms that it corresponds to the true minimum. However, due to the small S_1–S_0 gap calculated with the CI-singles method (0.29 and 0.21 eV for **1b** and **2b**, respectively), a twisted geometry cannot be responsible for the experimentally observed fluorescence (*ca.* 2.1 eV). Furthermore, nearly touching S_1 and S_0 potential energy surfaces are expected to result in a very short lifetime of the twisted state due to a highly efficient radiationless transition.

The failure to locate a fluorescent transient may be related to the limitations of the CI-singles method. However, as will be described below, even the considerably more sophisticated multiconfigurational self-consistent field (MCSCF) method gives a very similar description of the S_1 potential energy surface. It should be noted that, in principle, an emitting state might not necessarily be related to a minimum on a potential energy surface. It is not unreasonable that, on the picosecond timescale, even a non-Boltzmann population (*i.e.*, the molecules that are not in the potential energy well, but rather on the slope of the potential energy surface) can play an important role provided that the surface is sufficiently shallow. The vibrational relaxation path of the vertically excited dye molecule is therefore of considerable importance.

Hence, we set out to explore relaxation of the vertically excited state exemplified by **1a**. Based on the presence of a single minimum on the S_1 potential energy surface, vertical excitation should be followed by rapid barrierless relaxation to the twisted geometry, **1b**, and by a very rapid radiationless transition to the S_0 potential energy surface. Although the most striking difference between **1a** and **1b** is a 90° twist around the azomethine bond, an examination of the energy gradients, calculated for **1a** with the CI-singles method, indicates that the highest gradients correspond to the in-plane skeletal relaxation. Vanishingly small gradients correspond to the twisting of the arylamino fragment. A hypothetical trajectory for the relaxation of the vertically excited state may therefore be thought to consist of the two distinct stages schematically shown in Fig. 2: relatively rapid skeletal relaxation (**1a** $\longrightarrow$ **1c**) and relatively slow twisting of the arylamino fragment (**1c** $\longrightarrow$ **1b**). The **1c** point can be defined as a transition state between two enantiomeric twisted geometries, **1b**, or, in other words, as the highest point along a hypothetical twisting coordinate. It should be noted that some degree of twisting could be expected even for the population of the PT dye molecules in the ground state at ambient temperature. Following vertical excitation, such torsionally perturbed molecules should follow the trajectory shown with the dashed line in Fig. 2. This has been verified by demonstrating that a small twisting of the vertically excited state, **1a**, results in an energy decrease along with an increase in energy gradients corresponding to the further twisting of the arylamino fragment. Although the steepest descent path would

Table 1 Representative geometric parameters of **1** and **2** in ground and excited states at various levels of *ab initio* calculation. Distances are in Å and angles in degrees

Structure	Method	C1–C2–N3–C4	C2–N3–C4–C5	C6–C7–N8–C9	C2–N3–C4–C9	C2–N3	N3–C4	C4–C5	C5–C6	C6–C7	C7–C8
1a	RHF/6-31G*	−0.1	−0.1	−9.0	129.0	1.257	1.389	1.398	1.376	1.407	1.374
2a	RHF/6-31G*	0.0	−0.1	−7.8	129.4	1.257	1.388	1.394	1.375	1.406	1.372
1a′	MP2/6-31G*	−0.2	0.5	16.1	125.3	1.305	1.384	1.413	1.386	1.417	1.373
1a′′	B3LYP/6-31G*	0.0	0.0	0.0	127.4	1.296	1.376	1.419	1.382	1.421	1.374
1b	CIS/6-31G*	−95.0	1.7	1.7	129.0	1.316	1.339	1.412	1.369	1.413	1.359
2b	CIS/6-31G*	95.1	−1.4	−1.1	130.6	1.312	1.339	1.411	1.368	1.414	1.359
1c	CIS/6-31G*	0.0[a]	0.0[a]	0.0	126.1	1.327	1.331	1.435	1.364	1.418	1.353
2c	CIS/6-31G*	0.0[a]	0.0[a]	0.0	125.8	1.325	1.332	1.436	1.364	1.419	1.351
1c′	MCSCF(8e,8o)/6-31G*[b]	0.0[a]	180.0[a]	0.0	124.8	1.362	1.345	1.462	1.355	1.424	1.334

[a] Constrained angle. [b] Geometry optimization was performed for the second root (S_1 state).

Fig. 2 Hypothetical trajectories for the relaxation of excited singlet state of PT dyes. Bold and dashed lines exemplify relaxation of planar and partly twisted vertically excited dye molecules, respectively.

therefore never reach the **1c** point, it should still pass in its vicinity before any considerable twisting takes place. Thus, the shape of the potential energy surface corresponding to the twisting of the arylamino fragment is expected to play a decisive role on the rate at which the vibrational relaxation of PT dyes takes place. In the condensed phase the relative importance of the twisting should be even more prominent because, unlike the skeletal relaxation, it has a relatively large effect on the shape of the molecule and thereby requires considerable solvent reorganization. As a result, for the solvated molecules the average evolution time between the **1c** and **1b** points constitutes an even larger fraction of the total time spent on the S_1 potential energy surface.

In continuation of our efforts, we have performed a detailed study of the potential energy surface corresponding to the twisting of the arylamino fragment. In order to arrive at the **1c** geometry we initially performed the CI-singles geometry optimization of the **1a** structure with the azomethine double bond constrained at 0°. Interestingly, despite the constraint, the optimization still yielded a twisted structure due to the rotation around the C2–N3–C4–C5 single bond. Unlike the azomethine double bond rotation, this type of twisting leads only to a moderate energy lowering of the S_1 state. Despite the considerable change in the molecular geometry, the lowest transition remains dominated by a HOMO ⟶ LUMO single excitation. Calculated oscillator strength of this transition is nearly zero due to the HOMO and LUMO orbitals being orthogonal in the twisted structure.

Hence, both double and single bonds linking the PT and arylamino fragments appear to be important for the vibrational relaxation of the S_1 state of the PT dye. Both coordinates have been chosen to map the S_1 potential energy by means of the torsional driver technique. Dihedral angles C1–C2–N3–C4 and C2–N3–C4–C5 were stepped from −20° to 100° followed by complete geometry optimization with the CI-singles method. The resultant potential energy surface is shown in Fig. 3. A representative subset of the respective vertical excitation energies and oscillator strengths is given in Table 2. Vibrational analysis of the geometry obtained with the dihedral angles constrained at 0° showed a single imaginary frequency of 101.0 cm^{-1} corresponding to the twisting of the arylamino fragment. This geometry can therefore be identified with the postulated **1c** point. An interesting feature of **1c** is that it presents a striking quinoidal pattern in the aryl group. We also note a considerable lengthening of azomethine double bond C2–N3 and a shortening of the N3–C4 and C7–N8 single bonds. A hypothetical steepest descent path is shown with arrows in Fig. 3. In the vicinity of the **1c** point, this relaxation path involves a concerted rotational motion around the single and double bonds

Table 2 Results of the relaxed potential energy surface scan (CIS/6-31G*) as a function of dihedral angles (degrees) C1–C2–N3–C4 and C2–N3–C4–C5 of dye **1**. Total energies (in kJ mol^{-1}) are given relative to the planar geometry (**1c**, both dihedral angles are 0°), S_0–S_1 vertical excitation energies (in eV) are shown in parentheses, with the respective oscillator strengths in square brackets

	C1–C2–N3–C4										
C2–N3–C4–C5	−20	−10	0	10	20	30	50	70	80	90	100
−20	−36.9	−26.4	−14.0	−0.2	6.4	−5.1	−31.1	−55.6	−74.6	−89.1	−90.7
	(2.64)	(2.85)	(3.03)	(3.11)	(3.46)	(2.81)	(2.16)	(1.20)	(0.40)	(0.41)	(0.36)
	[0.37]	[0.42]	[0.44]	[0.34]	[1.30]	[0.29]	[0.23]	[0.07]	[0.003]	[0.000]	[0.000]
−10	−28.0	−15.8	−3.1	1.6	−4.1	−17.9	−40.9	−63.7	−81.7	−93.0	−93.6
	(2.78)	(3.02)	(3.45)	(3.51)	(3.05)	(2.74)	(2.06)	(1.07)	(0.30)	(0.34)	(0.31)
	[0.43]	[0.50]	[1.34]	[1.34]	[0.45]	[0.38]	[0.24]	[0.05]	[0.001]	[0.000]	[0.000]
0	−17.1	−4.2	0.0	−4.2	−17.1	−29.2	−49.0	−70.0	−85.2	−95.1	−93.7
	(2.91)	(3.40)	(3.53)	(3.40)	(2.91)	(2.63)	(1.95)	(0.99)	(0.35)	(0.29)	(0.30)
	[0.45]	[1.1]	[1.36]	[1.1]	[0.45]	[0.38]	[0.22]	[0.04]	[0.001]	[0.000]	[0.000]
10	−4.1	1.6	−3.1	−15.8	−28.0	−38.4	−55.3	−74.3	−86.3	−93.0	−91.0
	(3.05)	(3.51)	(3.45)	(3.02)	(2.78)	(2.51)	(1.82)	(0.95)	(0.46)	(0.34)	(0.32)
	[0.45]	[1.34]	[1.34]	[0.50]	[0.43]	[0.36]	[0.18]	[0.03]	[0.001]	[0.000]	[0.000]
20	6.4	−0.2	−14.0	−26.4	−36.9	−45.6	−60.2	−76.3	−85.1	−89.1	−85.3
	(3.46)	(3.11)	(3.03)	(2.85)	(2.64)	(2.39)	(1.71)	(0.95)	(0.55)	(0.41)	(0.34)
	[1.30]	[0.34]	[0.44]	[0.42]	[0.37]	[0.31]	[0.14]	[0.02]	[0.001]	[0.000]	[0.001]
30	0.9	−12.0	−24.3	−34.9	−43.6	−50.9	−63.6	−76.2	−81.4	−82.6	−76.7
	(3.00)	(2.99)	(2.84)	(2.68)	(2.48)	(2.23)	(1.59)	(0.95)	(0.65)	(0.49)	(0.40)
50	[0.23]	[0.37]	[0.37]	[0.35]	[0.30]	[0.24]	[0.09]	[0.01]	[0.001]	[0.000]	[0.001]
	−38.9	−31.2	−39.8	−46.9	−52.9	−57.8	−65.0	−67.7	−66.4	−61.8	−51.7
	(2.23)	(2.56)	(2.45)	(2.30)	(2.12)	(1.91)	(1.47)	(1.08)	(0.89)	(0.73)	(0.65)
70	[0.09]	[0.22]	[0.20]	[0.17]	[0.13]	[0.09]	[0.02]	[0.001]	[0.000]	[0.002]	(0.006]
	−52.3	−45.5	−50.8	−54.8	−57.4	−58.7	−56.9	−48.7	−42.1	−33.3	−21.5
	(1.93)	(2.17)	(2.08)	(1.97)	(1.86)	(1.76)	(1.56)	(1.34)	(1.23)	(1.14)	(1.13)
90	[0.01]	[0.08]	[0.06]	[0.04]	[0.02]	[0.01]	[0.000]	[0.01]	[0.01]	[0.01]	[0.02]
	−53.6	−55.5	−56.0	−55.5	−53.6	−50.1	−38.7	−22.5	−13.9	−6.7	−4.4
	(1.91)	(1.91)	(1.92)	(1.91)	(1.91)	(1.90)	(1.86)	(1.79)	(1.75)	(1.68)	(1.67)
	[0.005]	[0.001]	[0.000]	[0.001]	[0.005]	[0.01]	[0.03]	[0.04]	[0.03]	[0.01]	[0.001]

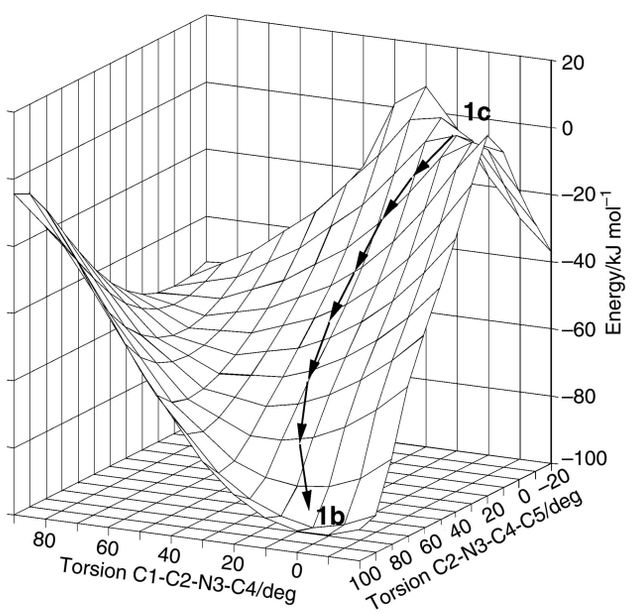

Fig. 3 Potential energy surface (CIS/6-31G*) as a function of dihedral angles C1–C2–N3–C4 and C2–N3–C4–C5 of dye **1**. Arrows represent a hypothetical relaxation path.

linking the PT and arylamino fragments. This has been confirmed by following the initial relaxation of **1c** with an IRC calculation.

An examination of the potential energy surface corresponding to the relaxation of the isomeric PT dye **2** yielded a very similar description. Interestingly, the CI-singles treatment predicts a steeper potential energy surface in the vicinity of the planar geometry: a 20° twist results in lower energies by 15.8 and 28.4 kJ mol^{-1} for the dyes **1** and **2**, respectively. The predicted steeper potential energy surface should result in faster transit towards a nonfluorescent twisted geometry. This is consistent with the lower quantum yields of fluorescence that we have generally observed for the dyes derived from the 7*H*-pyrazolo[1,5-*b*][1,2,4]triazole skeleton.

Table 3 Experimental λ_{max} (nm) of dye **1** in various solvents

Solvent	λ_{max}
Dimethylformamide	523
Methylene chloride	520
Acetonitrile	512
Acetone	512
Ethyl acetate	508
Toluene	508
Cyclohexane	498
Gas phase[a]	473

[a] Estimated according to ref. 16.

In good agreement with the results of conformational searching, a *barrierless* relaxation path of the S_1 state has been found. Although no spectroscopic minimum corresponding to the experimentally observed fluorescent state has been found along the path, sufficiently high values of oscillator strength (*cf.* Table 2) are computed even for the considerably twisted molecules along the relaxation path. Hence, CI-singles calculations predict the experimentally observed fluorescent state to correspond to the non-Boltzmann population of the PT dye molecules in transit on the S_1 potential energy surface.

The CI-singles method is known to provide a satisfactory zero-order description of numerous excited states.[9] It is generally expected to yield qualitatively correct results, particularly with respect to the potential energy surfaces calculations. Given an appropriate choice of the basis set, the vertical excitation energies of many simple molecules have been calculated quite accurately. This may serve as a possible test of whether the CI-singles technique is suitable to describe excited states for the molecule of interest. For the PT dyes, we have seen only a relatively poor agreement between the experimental and calculated excitation energies. Table 3 lists the experimental λ_{max} of **1a** in different solvents. Estimated from the solution data, the gas

Table 4 S_0–S_1 vertical excitation energies (eV) of dye **1** at various levels of *ab initio* calculation

Geometry	Method	Excitation energy	MCQDPT corrected energy
1a	CIS/6-31G*	4.27	
1a′	CIS/6-31G*	3.84	
1a′′	CIS/6-31G*	3.86	
1a	CIS/6-31+G*	4.32	
1a	CIS/6-31++G**	4.36	
1a	MCSCF(4e,4o)/6-31G*	4.39	3.00
1a	MCSCF(6e,6o)/6-31G*	4.49	3.18
1a	MCSCF(8e,8o)/6-31G*	4.61	3.07
1a	MCSCF(10e,10o)/6-31G*	4.69	3.25
1a′	MCSCF(8e,8o)/6-31G*	4.27	2.79

Table 5 Results of the relaxed potential energy surface scan (MCSCF(8e,8o)/6-31G*) as a function of dihedral angles C1–C2–N3–C4 and C2–N3–C4–C5 of dye **1**. Total energies (kJ mol^{-1}) are given relative to the planar geometry (**1c′**, both dihedral angles are 0°)

C1–C2–N3–C4	C2–N3–C4–C5	Total energy/kJ mol^{-1}	S_0–S_1 vertical excitation energy/eV	S_0–S_1 transition oscillator strength
0	0	0	3.55	0.923
10	0	−0.37	3.47	0.915
0	10	0.32	3.57	0.885
10	10	−1.11	3.47	0.857
10	−10	1.17	3.54	0.908
20	0	−2.58	3.00	0.807
0	20	0.16	3.62	0.751
20	20	−4.08	3.38	0.669

phase excitation energy[16] of 2.6 eV does not agree well with the value of 4.27 eV calculated with the CI-singles method using the 6-31G* basis set. As shown in Table 4, addition of the diffuse function afforded no improvement. The observed large discrepancy between the calculated and experimental vertical excitation energies is unlikely to be due to the incorrect ground state geometry. As shown in Table 4, ground state geometries generated by several higher level *ab initio* methods, including treatment of the correlation effects, also yielded unrealistically high vertical excitation energies. Most likely, the origin of the discrepancy lies in the inherent limitations of the CI-singles method, particularly when applied to π–π* transitions that are difficult to calculate accurately.[17] Multiconfigurational self-consistent field (MCSCF) calculations are generally expected to provide a more realistic description of the excited states due to the inclusion of multiple excitations and the refinement of the excited state wavefunction. Although there are no experimental data pertaining to the twisted geometry such as **1b**, the shortcomings of the CI-singles method should be even more pronounced as the single determinant HF treatment may not be appropriate to generate a reference wavefunction corresponding to a biradicaloid structure.

Somewhat unexpectedly, an application of the MCSCF method to the **1a** geometry did not yield any improvement in computed excitation energies shown in Table 4. Similarly to CI-singles, MCSCF calculations predicted the lowest transition to have a π–π* nature and high oscillator strength. Regardless of the active space choice, the MCSCF wavefunction of the S_1 state is dominated by a single excitation HOMO ⟶ LUMO. This lends additional credibility to a qualitative description of the S_1 potential energy surface obtained at the CI-singles level.

Inclusion of the dynamic correlation effects *via* perturbational theory, as implemented by the MCQDPT method of Gamess, led to a considerably better agreement with the estimated gas phase vertical excitation energy. Next, an application of the MCQDPT method to the ground state geometry optimized at the MP2/6-31G*level yielded the computed excitation energy within 0.2 eV of the experimental value. Thus, correlation effects appear essential for the accurate characterization of the S_1 state of the PT dyes. Following this lead, we have set out to reexamine the relaxation of the S_1 state of the representative PT dye with the MCSCF method. Due to the considerable computational expense of this method, we have confined our investigation to those two regions of the potential energy surface that are of particular interest as judged from the CI-singles study: the region in the vicinity of the planar geometry, presumably corresponding to the fluorescent transient, and the region of the twisted geometry, corresponding to the smallest separation between the S_1 and S_0 potential energy surfaces. Based on the results of the single point calculations shown in Table 4, an active space of eight electrons in eight orbitals (8e,8o) was chosen for the subsequent geometry optimizations as a reasonable compromise between performance and accuracy.

As with the CI-singles method, we have located the transition state, **1c′**, corresponding to the twisting of the arylamino fragment, by performing a geometry optimization with dihedral angles C1–C2–N3–C4 and C2–N3–C4–C5 constrained at 0°. Vibrational analysis of **1c′** showed a single imaginary frequency of 48.6 cm^{-1}, a somewhat smaller value compared to the CI-singles method. The results of the several constrained optimizations are shown in Table 5 and the following is noteworthy. Qualitatively, the MCSCF S_1 potential energy surface is very similar to the one obtained with the CI-singles method. Here again, a hypothetical relaxation path is likely to involve a concerted rotation of the double and single bonds linking the PT and arylamino fragments. However, the MCSCF method predicts the surface to be considerably more shallow: a 20° twist results in energy lowering by *ca*. 15.8 and 1.1 kJ mol^{-1} for the CI-singles and MCSCF methods, respectively. Although considerably more shallow, the MCSCF description of the S_1 potential energy surface still does not yield any spectroscopic minima. All geometries that were obtained in constrained minimizations underwent further twisting when the constraints were lifted. By analogy with the CI-singles method it may be expected that the actual S_1 minimum corresponds to the twisted geometry. Unfortunately, we could not follow relaxation of the **1a** geometry all the way to a hypothetical twisted minimum because of the loss of MCSCF convergence for the twist angles larger than 50–60°. The loss of convergence is due to the non-ideal method applied to the excited state calculation.[18] As the twist angle increases, the separation between the two lowest roots becomes smaller. As a result, at a certain twist angle, the excited state orbital optimization process results in the

approximate ground state energy increase until it approaches the excited state energy. At this point, the wavefunction becomes undefined within the degenerate space. This behavior is an artifact of the MCSCF model and can be avoided by using state averaging. However, Gamess implementation of the state averaging precludes calculation of the energy gradients and, therefore, geometry optimizations.

In order to obtain MCSCF description of the S_1 and S_0 states in the region of the twisted geometry, we have started with the state averaged calculation on the **1b** geometry using an active space of 26 electrons in 20 orbitals, while restricting the maximum excitation level to triples. Such an active space was chosen to allow inclusion of all p and n orbitals. Unfortunately, RHF orbitals (normally used as a starting guess) were highly contaminated with σ character. This led to considerable difficulties in achieving MCSCF convergence. Although we have not performed exhaustive studies, our experience suggests that the "complete" active space (*i.e.*, potentially including all p and n orbitals) is important to converge the MCSCF wavefunction for structures such as **1b**. Interestingly, examination of the converged MCSCF orbitals shows that all σ character has been eliminated. Using these orbitals as a starting guess allowed us to achieve MCSCF convergence for the (8e,8o) active space with the unrestricted maximum excitation level for the S_0 and S_1 states. The calculated S_1–S_0 gap is 0.01 eV, which is considerably less than the value calculated with the CI-singles method. Examination of the calculated state properties suggests that the crossing between the S_0 and S_1 potential energy surfaces has occurred somewhere along the twisting coordinate. Contrary to the CI-singles method description, MCSCF calculations predict that, at the **1b** geometry, the lowest state has a higher dipole moment (8.4 D), and is dominated by HOMO ⟶ LUMO single excitation (69%). On the other hand, the S_1 state is calculated to have a lower dipole moment (4.8 D) and is dominated by the ground state configuration (64%). After introducing MCQDPT corrections, the crossing between the S_0 and S_1 potential energy surfaces along the twisting coordinate is even more apparent: the calculated S_1–S_0 gap is 0.9 eV.

Subsequent geometry optimizations of both states at the MCSCF level yielded the very same planar ground state geometry. Lack of a discernible minimum in the vicinity of the twisted geometry is consistent with the presence of a peaked conical intersection.[19] Although we have not characterized the respective conical intersection thus far, there is little doubt that the relaxation path of the fluorescent transient occurs along the twisting coordinate until it encounters unavoided crossing with the ground state potential energy surface. Formation of the transient (nonfluorescent or fluorescent) with a twisted geometry and appreciable lifetime is therefore unlikely.

Although the CI-singles method fails to capture S_0–S_1 state crossing, it appears that the CI-singles and MCSCF methods provide a qualitatively similar description of the S_1 state potential energy surface along the relaxation coordinate. Both methods predict the fluorescent transient to correspond to a non-Boltzmann population of the PT dye molecules in a barrierless transit on the S_1 potential energy surface towards a nonfluorescent twisted geometry. These results, along with the predicted relatively shallow MCSCF potential energy surface around the planar geometry, have focused our attention on this region. The predicted barrierless nature of the relaxation path of the fluorescent transient may be expected to have a number of consequences such as a very short lifetime and nonmonoexponential decays observed by time-resolved emission and absorption spectroscopy. As discussed in the Introduction, this is indeed the behavior observed for a number of the representative PT dyes. However, this agreement between the experimental observations and theoretical predictions should not be taken too enthusiastically. Many different explanations may be envisioned to accommodate these experimental observations.[6]

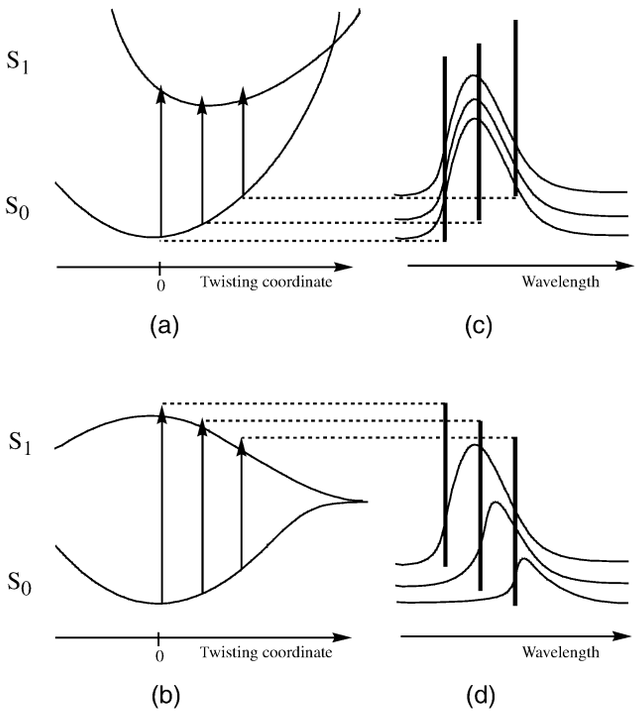

Fig. 4 Anticipated effects of the shape of potential energy surface [classical excited state and non-Boltzmann population are exemplified by (a) and (b), respectively] on emission spectra [classical fluorescence behavior and strong excitation wavelength dependence of fluorescence are shown as (c) and (d), respectively]. Vertical bars denote excitation wavelengths.

On the other hand, the barrierless nature of the fluorescent state relaxation implies that the dissimilar initial populations should not necessarily yield identical emission spectra. Indeed, excited molecules only have a chance to fluoresce from the non-equilibrium state. They do not reach a common spectroscopic minimum on the potential energy surface due to the lack of such a minimum. In principle, excitation with the different wavelengths of monochromatic light may be expected to yield populations sufficiently different as to be distinct in steady state fluorescence experiments. Considering the small Stokes shift normally observed for the PT dyes, this effect should be quite pronounced for excitation wavelengths longer than the maximum of the absorption band. Indeed, given the characteristics of the computed S_1 potential energy surface, most of the emission band may be expected to remain at the longer wavelengths relative to the excitation light. Thereby, beyond a certain point, a shift of the excitation towards longer wavelengths should result in an emission band shift of at least equal magnitude. Additionally, because of the decrease in the oscillator strength associated with twisting (Table 2), a corresponding decrease in the relative fluorescence quantum yield may also be expected. As illustrated in Fig. 4, this behavior is in sharp contrast with classical fluorescence behavior. Indeed, it has been known for more than a century that the solution fluorescence spectra of a single component do not depend on the frequency of the excitation light. At the present time this notion appears still very well justified, with only a few cases of nonclassical behavior being documented where a high solvent viscosity[20] or a very short fluorescence decay time[21] has led to a certain dependence of the fluorescence spectrum on the frequency of the excitation light. The origin of the nonclassical behavior is generally attributed to the reorientation of polar solvent molecules being slow relative to the fluorescence decay time. However, as illustrated in Fig. 4, the origin of the predicted nonclassical behavior of PT dyes is quite different. If our description of the S_1 potential energy surface is qualitatively correct, the fluorescence of PT dyes is to be expected to exhibit comparable excitation wave-

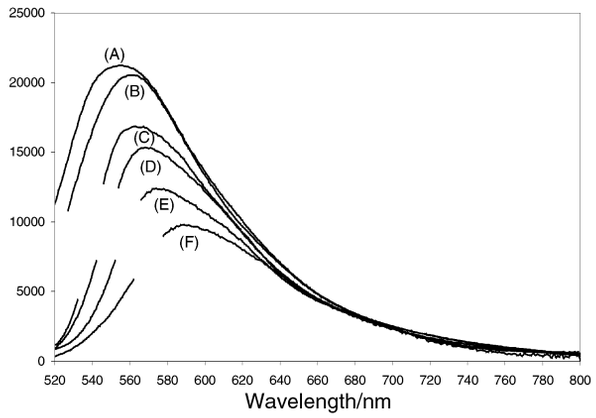

Fig. 5 Emission spectra of **1** in ethyl acetate as a function of excitation wavelength: (A) 500, (B) 520, (C) 540, (D) 550, (E) 560, and (F) 570 nm.

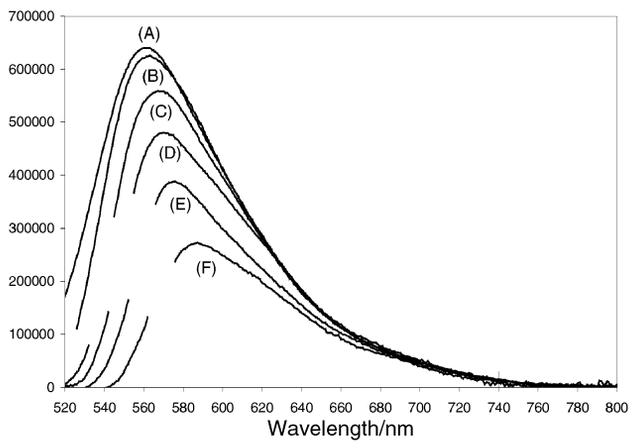

Fig. 6 Emission spectra of **1** in sucrose octaacetate as a function of excitation wavelength: (A) 500, (B) 520, (C) 540, (D) 550, (E) 560, and (F) 570 nm.

length dependence regardless of the solvent properties. The origin of the wavelength effect is intrinsic to the structure of the PT dye. To our best knowledge such behavior is unprecedented and, therefore, presents an excellent opportunity to assess the realism of the computational model.

The study of the fluorescence spectra as a function of the excitation wavelength was performed using dilute solutions (*ca.* 3.0×10^{-6} M) of dye **1** in ethyl acetate and sucrose octaacetate at room temperature. Sucrose octaacetate was chosen for this study because it is a highly viscous solvent with the appearance of rigid glass at room temperature, yet it is fairly similar to ethyl acetate with respect to its polarity. The possible involvement of concentration effects caused by aggregation or energy transfer was probed by means of collecting fluorescence spectra of several samples with concentrations in the range 10^{-5}–10^{-6} M. As judged from the observation of the superimposable emission spectra after correcting them for the difference in absorbance, the chosen concentration is sufficiently low to consider the experimental solutions infinitely dilute. Figs. 5 and 6 show the emission spectra as a function of the excitation wavelength in the 500–570 nm range after correcting them for the differences in absorbance. Only minor changes of the emission spectrum profile were observed with the excitation wavelengths shorter than 500 nm.

Consistent with the previous observations,[6] a solvent of higher viscosity causes nearly a 30-fold increase in fluorescence intensity. Although there are certain subtle changes in the shape of the fluorescence spectra between the two solutions, it is quite remarkable that they exhibit nearly the same effect as the excitation wavelength. In excellent agreement with the predictions, regardless of the solvent viscosity, excitation with longer wavelengths results in a considerable shift of the emission band along with a decrease in relative fluorescence quantum yield. It is instructive to note that the observed decrease in the fluorescence quantum yield at longer excitation wavelengths effectively eliminates any possibility of an involvement of a fluorescent impurity in the observed behavior. Indeed, the involvement of a fluorescent impurity at the longer excitation wavelengths is to be expected to result in an increase in the fluorescence quantum yield, which is contrary to the experimental observations. A similar conclusion has been reached after examination of the excitation spectra as a function of the emission wavelength. As the observation wavelength was varied from 550 to 600 nm, the respective maxima of the excitation spectra remained within 2 nm of the absorption spectrum maximum.

Several conclusions can be drawn from the present study. The good agreement between the experiment and extensive *ab initio* modeling of the excited states of PT dyes highlights the value of the computational models in predicting actual chemical behavior, even in a relatively difficult case such as that of the chemistry of excited states. Our results strongly suggest that the fluorescent transient is, in fact, a non-Boltzmann population of the hot molecules in the S_1 electronic state. The non-Boltzmann nature of the fluorescent transient is a consequence of the existence of a barrierless relaxation path leading towards a S_1–S_0 crossing, which corresponds to the twisted geometry. The shape of the potential energy surface along the predicted relaxation path not only explains the unprecedented wavelength effects reported in this study, but also is in excellent agreement with the low quantum yields and nonexponential decays of fluorescence generally observed for PT dyes.[2,6]

Acknowledgements

The author is grateful to Dr Kris Krishnamurthy for support and encouragement and to Dr Faraj Abu-Hasanayn, Dr Leif Olson, and Dr David Giesen for fruitful discussions. Dr John Harder is thanked for reviewing the manuscript.

References

1 J. Bailey, *J. Chem. Soc., Perkin Trans. 1*, 1977, 2047.
2 K. Furuya, N. Furutachi, S. Oda and K. Maruyama, *J. Chem. Soc., Perkin Trans. 2*, 1994, 531.
3 R. Jain, R. P. Scaringe and M. McMillan, personal communication.
4 J. McKelvey, personal communication.
5 P. Douglas, *J. Photogr. Sci.*, 1988, **36**, 83.
6 P. Douglas, S. M. Townsend, P. J. Booth, B. Crystall, J. R. Durrant and D. R. Klug, *J. Chem. Soc., Faraday Trans.*, 1991, **87**, 3479.
7 J. R. Lakowicz, *Principles of Fluorescence Spectroscopy*, Plenum Press, New York, 1983, p. 58.
8 F. Wilkinson, D. R. Worall and R. S. Chittock, *Chem. Phys. Lett.*, 1990, **174**, 416; F. Wilkinson, D. Worall, D. McGarvey, A. Goodwin and A. Langloy, *J. Chem. Soc., Faraday Trans.*, 1993, **89**, 2385.
9 J. B. Foresman, M. Head-Gordon, J. A. Pople and M. J. Frisch, *J. Phys. Chem.*, 1992, **96**, 135 and references therein; J. Paldus and X. Li, *Adv. Chem. Phys.*, 1999, **110**, 1 and references therein.
10 M. Klessinger and J. Michl, *Excited States and Photochemistry of Organic Molecules*, VCH Publishers, New York, 1995.
11 T. Oshiyama, S. Daiba, H. Iizuka and F. Ishii, *Nippon Shashin Gakkaishi*, 1995, **58**, 129.
12 L. Olson and D. Giesen, personal communication.
13 M. W. Schmidt, K. K. Baldridge, J. A. Boatz, S. T. Elbert, M. S. Gordon, J. J. Jensen, S. Koseki, N. Matsunaga, K. A. Nguyen, S. Su, T. L. Windus, M. Dupuis and J. A. Montgomery, *J. Comput. Chem.*, 1993, **14**, 1347.
14 A. A. Granovsky, http://classic.chem.msu.su/gran/gamess/index.html.
15 Gaussian 98, Revision A. 6, M. J. Frisch, G. W. Trucks, H. B. Schlegel, G. E. Scuseria, M. A. Robb, J. R. Cheeseman, V. G. Zakrzewski, J. A. Montgomery, Jr., R. E. Stratmann, J. C. Burant, S. Dapprich, J. M. Millam, A. D. Daniels, K. N. Kudin, M. C. Strain, O. Farkas, J. Tomasi, V. Barone, M. Cossi, R. Cammi, B. Mennucci, C. Pomelli, C. Adamo, S. Clifford, J. Ochterski, G. A. Petersson, P. Y. Ayala, Q. Cui, K. Morokuma, D. K. Malick, A. D. Rabuck,

K. Raghavachari, J. B. Foresman, J. Cioslowski, J. V. Ortiz, B. B. Stefanov, G. Liu, A. Liashenko, P. Piskorz, I. Komaromi, R. Gomperts, R. L. Martin, D. J. Fox, T. Keith, M. A. Al-Laham, C. Y. Peng, A. Nanayakkara, C. Gonzalez, M. Challacombe, P. M. W. Gill, B. Johnson, W. Chen, M. W. Wong, J. L. Andres, M. Head-Gordon, E. S. Replogle and J. A. Pople, Gaussian, Inc., Pittsburgh PA, 1998.

16 M. Essfar, G. Guiheneuf and J.-L. M. Abboud, *J. Am. Chem. Soc.*, 1982, **104**, 6786; J.-L. M. Abboud, G. Guiheneuf, M. Essfar, R. W. Taft and M. J. Kamlet, *J. Phys. Chem.*, 1984, **88**, 4414.

17 M. Klessinger and J. Michl, *Excited States and Photochemistry of Organic Molecules*, VCH Publishers, New York, 1995, p. 60.

18 R. Shepard, *Adv. Chem. Phys.*, 1987, **69**, 80.

19 G. J. Atchity, S. S. Xantheas and K. Ruedenberg, *J. Chem. Phys.*, 1991, **95**, 1862.

20 N. G. Bakhshiev, Y. T. Mazurenko and I. V. Piterskaya, *Opt. Spektrosk.*, 1966, **21**, 307 and references therein; W. R. Ware, S. K. Lee, G. J. Brant and P. P. Chow, *J. Chem. Phys.*, 1971, **54**, 4729; A. Kawski and J. Kukielski, *J. Lumin.*, 1971, **4**, 155; K. A. Al-Hassan and M. A. El-Bayoumi, *Chem. Phys. Lett.*, 1980, **76**, 121; S. Kinoshita, N. Nishi and T. Kushida, *Chem. Phys. Lett.*, 1987, **134**, 605; A. Stein and M. D. Fayer, *Chem. Phys. Lett.*, 1991, **176**, 159.

21 A. Kawski, *Z. Naturforsch., A: Phys. Phys. Chem. Kosmophys.*, 1984, **39**, 509; A. Baczynski, M. Czajkowski and B. Zietek, *J. Fluoresc.*, 1993, **3**, 17.